

Adversarial Attacks and Defenses for Speaker Identification Systems

Sonal Joshi, *Student Member*, Jesús Villalba, *Member, IEEE*, Piotr Żelasko, *Member, IEEE*, Laureano Moro-Velázquez, *Member, IEEE*, and Najim Dehak, *Senior Member, IEEE*

Abstract—Research in automatic speaker recognition (SR) has been undertaken for several decades, reaching great performance. However, researchers discovered potential loopholes in these technologies like spoofing attacks—voice replay, conversion, and synthesis— and thoroughly investigated them in the last years. Quite recently, a new genre of attack, termed adversarial attacks, has been proved to be fatal in computer vision (CV), and it is vital to study their effects on SR systems. This paper examines how state-of-the-art speaker identification (SID) systems are vulnerable to adversarial attacks and how to defend against them. We investigated adversarial attacks common in the literature like fast gradient sign method (FGSM), iterative-FGSM—a.k.a. basic iterative method (BIM)—, and Carlini-Wagner (CW). Furthermore, we propose four pre-processing defenses against these attacks—viz. randomized smoothing, DefenseGAN, variational autoencoder (VAE), and WaveGAN vocoder. We found that SID were extremely vulnerable under Iterative FGSM and Carlini-Wagner attacks. Randomized smoothing defense robustified the system for imperceptible BIM and Carlini-Wagner attacks recovering classification accuracies $\sim 97\%$. Defenses based on generative models (DefenseGAN, VAE, and WaveGAN) project adversarial examples (outside of the manifold) back into the clean manifold. In the case that the attacker cannot adapt the attack to the defense (black-box defense), WaveGAN performed the best, being close to the clean condition (Accuracy $> 97\%$). However, if the attack is adapted to the defense—assuming the attacker has access to the defense model—(white-box defense), VAE and WaveGAN protection dropped significantly—50% and 37% accuracy for CW attack. To counteract this, we combined randomized smoothing with VAE or WaveGAN. We found that smoothing followed by WaveGAN vocoder was the most effective defense overall. As a black-box defense, it provides 93% average accuracy. A white-box defense, accuracy only degraded for iterative attacks with perceptible perturbations ($L_\infty \geq 0.01$).

Index Terms—Speaker Recognition, x-vectors, adversarial attacks, adversarial defenses

I. INTRODUCTION

SPEAKER recognition (SR) has application in forensics, smart home assistants, authentication, etc. Recently, research has shown that these systems are subject to threats, including spoofing and adversarial attacks [1]. Spoofing has been extensively studied in ASVSpooF challenges [2], and

countermeasures have been proposed [3]. However, the adversarial attacks field remains less explored. SR adversarial attacks usually consist of slightly modifying the original signal by adding a small human-imperceptible noise to make the SR neural network fail and give incorrect predictions [4]. The question is how effective are these attacks and how we defend against them.

As the pioneering work on adversarial attacks was in the area of image classification [4], attacks to computer vision systems have been extensively studied [5], [6], [7], [8]. These attacks have been, later, extended to other modalities like video [9] and speech. For the latter, adversarial attacks have been studied for Automatic speech recognition systems (ASR) and speaker recognition (SR). Adversarial attacks on ASR are generally focused on end-to-end architectures, e.g., Mozilla’s DeepSpeech [10], rather than hybrid DNN-HMM systems. For example, the study in [11] attacks DeepSpeech using Houdini attack. Another study [12] proposes a white-box iterative optimization-based adversarial attack (henceforth referred to as Carlini-Wagner attack), demonstrating a 100% success rate. The authors in [13] propose an audio-agnostic universal adversarial perturbation for DeepSpeech. The authors in [14] attack WaveNet [15] using fast gradient sign method [16] and the fooling gradient sign method [4]. On the other hand, some works attack the state-of-the-art ASR based on Kaldi [17]. The authors in [18] propose a surreptitious attack to a Kaldi based ASR by embedding voice into songs and playing it in the background while being inaudible to the human ear. The studies [19], [20] show that psychoacoustic modeling can be leveraged to make the attacks imperceptible. Some other works [20], [21] suggest that physical adversarial attacks, meaning adversarial attacks generated over-the-air using realistic simulated environmental distortions, also break ASR system. More detailed overview of adversarial attacks and countermeasures on ASR is presented in [22].

Another speech technology under the radar of adversarial attacks is speaker recognition (SR) which is an umbrella term for three areas: speaker identification or classification (given a voice, identify who is speaking), speaker verification (given a voice and a claimed identity, decide whether the claim is correct or not), and anti-spoofing (spoofing countermeasures for replay, voice-synthesis attacks on speaker verification systems). The adversarial attacks research in the SR field started on non-state-of-the-art speaker identification systems. For instance, authors in [23], [24] attack models based on recurrent Long Short Term Memory (LSTM). Recently, a handful of works focusing on attacking on state-of-the-art

All authors are associated with the Department of Electrical and Computer Engineering, and the Center for Language and Speech Processing (CLSP), Johns Hopkins University, Baltimore, MD, 21218 USA

Jesús Villalba and Najim Dehak are also affiliated to the Human Language Technology Center of Excellence, Johns Hopkins University, Baltimore, MD, 21218, USA

This project was supported by DARPA Award HR001119S0026-GARD-FP-052

Manuscript received January xx, 2021

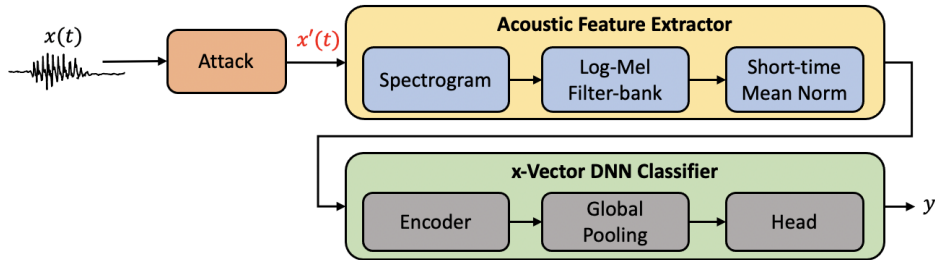


Fig. 1: x-Vector Speaker Classification Pipeline. Here, x' is adversarial sample of benign waveform x (with without attack gives classifier output as speaker label y^{benign}) such that the classifier output is y^{adv} (or in short y) such that $y \neq y^{\text{benign}}$

x-vector [25] and i-vector [26] systems are available in the literature. [27] attacks GMM i-vector and x-vector models using Fast Gradient Sign Method (FGSM). [28] attacks a public pre-trained Kaldi time-delay neural network (TDNN) based x-vector model by proposing a real-time black-box universal attack. Authors in [29] introduce universal adversarial perturbations (UAP) that can fool SR systems with high probability using generative networks to model the low-dimensional manifold of UAPs. The study [30] proposes a white-box psychoacoustics-based method to attack an x-vector model. A recent survey study [31] provides a good overview of existing research in this area and claims that the attacks “almost universally” fail to transfer to other models. Authors in [32] study the effects of adversarial attacks on speaker verification x-vector systems. They successfully transfer white-box attacks like FGSM, randomized FGSM and CW from small white-box to larger black-box systems. [33] proposes a Momentum Iterative Fast Gradient Sign Method (MI-FGSM) attack against spoofing countermeasure systems.

The question that arises is if there is a way to defend against adversarial attacks. As attack algorithms rely on the classifier’s gradient information, gradient masking/obfuscation can be used as a defense. For example, authors of [34] use defensive distillation when training DNNs to defend against adversarial attacks; and [35], [36] use pre-processing of input data by adding a non-smooth or non-differentiable preprocessor. PixelDefend [37] and Defense-GAN [38] use generative models to project adversarial samples onto the clean/benign manifold. PixelDefend uses the PixelCNN model and Defense-GAN uses a generative adversarial network to do the projection. Adding the generative network before the classifier causes the final model to be an extremely deep neural network, and hence the cumulative gradient to be extremely small or irregularly large [9]. This makes estimating the gradient difficult. Another type of defense is to make the model inherently robust against adversarial attacks. This can be done is by introducing adversarial samples in model training. This method is called adversarial training. The authors of [39] and [40] propose adversarial training using FGSM attacks, and those of [41] use projected gradient descent (PGD) attacks. PGD adversarial training generalizes better for unseen attacks than FGSM; however, it’s computationally costly and hence slow. [42] proposes “You Only Propagate Once” (YOPO) algorithm to make adversarial training faster by reusing gradients while generating PGD attacks. Some defenses called “certified

defenses” guarantee protection up to a certain perturbation L_p radius [43], [44]

For SR and ASR systems, pre-processing and adversarial training defenses are also found in the literature. In the class of pre-processing defenses, audio turbulence and audio squeezing have been proposed for ASR defense in [18]. Another study [45] proposes local smoothing using a low-pass filter, down-sampling/up-sampling, and quantization. The research for defenses for SR has been sparse. Some authors propose MP3 compression [46], whereas others employ a separate VGG-like binary classifier to detect the attacks [47]. Recently, the study [48] proposes adversarial training based on Projected Gradient Descent (PGD) attacks. Another work [49] proposes a defense mechanism based on a hybrid adversarial training using multi-task objectives, feature-scattering (FS), and margin losses. However, the caveats of adversarial training are that generalizes poorly to attack algorithms and threat models unseen during training, and requires careful training hyperparameter tuning besides significantly increasing training time. Given these issues, our work focuses on the class of pre-processing defenses. The main advantage of these defenses is that they do not need information about the type of attacks used by the adversary.

The main contributions of this work are as follows:

- We evaluate the performance of four attacks at various strengths on state-of-the-art speaker identification or classification model (x-vector) and show its vulnerability to adversarial attacks.
- We analyze four pre-processing defenses—viz. randomized smoothing defense (Section V-A), Defense-GAN (Section V-B), variational auto-encoder (VAE) defense (Section V-C) and WaveGAN vocoder defense (Section V-D). The first two are adapted from computer vision literature and the last two are newly proposed in this paper.
- We show that while the x-vector system has inherent robustness against some attacks like transfer universal attacks and low L_∞ FGSM attacks, defenses like WaveGAN vocoder and VAE help the x-vector to withstand more stronger attacks.

The rest of the paper is organized as follows: Section II describes the x-vector Speaker classification network; Section III describes the considered threat model; Section IV formally introduces adversarial attacks and methods; Section V describes proposed defense methods against the adversarial

TABLE I: ThinResNet34 x-vector architecture. N in the last row is the number of speakers. The first dimension of the input shows number of filter-banks and the third dimension indicates the number of frames T .

Layer name	Structure	Output
Input	–	$80 \times 1 \times T$
Conv2D-1	$3 \times 3, 16, \text{Stride } 1$	$80 \times 16 \times T$
ResNetBlock-1	$\begin{bmatrix} 3 \times 3, 16 \\ 3 \times 3, 16 \end{bmatrix} \times 3, \text{Stride } 1$	$80 \times 16 \times T$
ResNetBlock-2	$\begin{bmatrix} 3 \times 3, 32 \\ 3 \times 3, 32 \end{bmatrix} \times 4, \text{Stride } 2$	$40 \times 32 \times T/2$
ResNetBlock-3	$\begin{bmatrix} 3 \times 3, 64 \\ 3 \times 3, 64 \end{bmatrix} \times 6, \text{Stride } 2$	$20 \times 64 \times T/4$
ResNetBlock-4	$\begin{bmatrix} 3 \times 3, 128 \\ 3 \times 3, 128 \end{bmatrix} \times 3, \text{Stride } 2$	$10 \times 128 \times T/8$
Flatten	–	$1280 \times T/8$
StatsPooling	–	2560
Dense1	–	256
Dense2 (Softmax)	–	N

attacks; Section VI shows the experimental setup and the results are discussed in Section VII; and finally, Section VIII gives concluding remarks.

II. X-VECTOR SPEAKER CLASSIFICATION

In this study, we used state-of-the-art *x-vector* style neural architectures [50], [25] for the Speaker Classification task. x-Vector networks are divided into three parts. First, an encoder network extracts frame-level representations from acoustic features such as MFCC or filter-banks. Second, a global temporal pooling layer that aggregates the frame-level representation into a single vector per utterance. We used mean and standard deviation over time for pooling. Finally, a classification head, which is a feed-forward classification network, processes this single vector and computes the speaker class posteriors. This network is trained using additive angular margin softmax (AAM-softmax) [51] loss. Different x-vector systems are characterized by different encoder architectures, pooling methods, and training objectives. In preliminary experiments, we compared the vulnerability of x-vectors based on ThinResNet34, ResNet34 [52], [53], EfficientNet [54] and Transformer [55] Encoders to adversarial attacks. These results are shown in Section VII-A. We found that all architectures were similarly vulnerable, being EfficientNet slightly more robust for some attacks. To evaluate the defenses, we used the ThinResNet34 x-vector, whose architecture is described in Table I. ThinResNet34 was more vulnerable than the larger EfficientNets and ResNets, so we will be able to observe the defense improvement better. Also, it allowed us to reduce the computing cost. Having a small computing cost is very important since generating attacks involves multiple gradient descend iterations per trial.

III. THREAT MODEL

We consider a threat model where an attacker crafts an adversarial example by adding an imperceptible perturbation to the speech waveform in order to alter the speaker identification decision. Suppose $\mathbf{x} \in \mathbb{R}^T$ is the original clean audio waveform of length T , also called benign, or bonafide. Let y^{benign}

be its true label. Let $g(\cdot)$ be the x-vector network predicting speaker class posteriors. An adversarial example of \mathbf{x} is given by $\mathbf{x}' = \mathbf{x} + \delta$, where δ is the adversarial perturbation.

δ can be optimized to produce untargeted or targeted attacks. Untargeted attacks make the system to predict any class other than the true class, $g(\mathbf{x}') \neq y^{\text{benign}}$, but without forcing to predict any specific target class. On the contrary, targeted attacks are successful only when the system predict a given target class y^{adv} instead of the true class, $g(\mathbf{x}') = y^{\text{adv}} \neq y^{\text{benign}}$. In this work, we consider untargeted attacks since we observed that it is easier to make them succeed. Thus, we expect that defending from those attacks will be more difficult.

To enforce imperceptibility of the perturbation, some distance metric is minimized or bounded $D(\mathbf{x}, \mathbf{x}') < \varepsilon$. Typically, this is the L_p norm of the perturbation, $D(\mathbf{x}, \mathbf{x}') = \|\delta\|_p$. Among the attacks that we considered, FGSM and Iter-FGSM attacks limit the maximum L_∞ norm, while Carlini-Wagner minimizes the L_2 norm.

We considered two variants of this threat model depending on the knowledge of the attacker: white-box and black-box attacks. In white-box attacks, the attacker has fullknowledge of the system, including the architecture and parameters. They can compute the gradient of the loss function and back-propagate it all the way to the waveform to compute the adversarial perturbation. We performed experiments with three attacks in white-box settings: Fast Gradient Sign (FGSM) [5] (Section IV-A), Iterative FGSM [7] (Section IV-B) and Carlini-Wagner [6] (Section IV-C) attacks.

In black-box attacks, the attacker does not have details about the architecture of the x-vector system, and the adversary can just observe the predicted labels of the system given an input. In this work, we consider a particular case of black-box attack, usually known as *transfer based black-box attack*. Here, the idea is that the adversary has access to an alternative white-box model, which he can use to create adversarial examples, and use them to attack the victim model.

IV. ADVERSARIAL ATTACKS

Following, we describe the attack algorithms that we evaluated.

A. Fast gradient sign method (FGSM)

Fast gradient sign method (FGSM) [5] takes the benign audio waveform of length T $\mathbf{x} \in \mathbb{R}^T$ and computes an adversarial example \mathbf{x}' by taking a single step in the direction that maximizes the missclassification error as

$$\mathbf{x}' = \mathbf{x} + \varepsilon \text{sign}(\nabla_{\mathbf{x}} L(g(\mathbf{x}), y^{\text{benign}})), \quad (1)$$

where function $g(\mathbf{x})$ is the x-vector network producing speaker label posteriors, L is categorical cross-entropy loss, y^{benign} is the true label of the utterance. ε restricts the L_∞ norm of the perturbation by imposing $\|\mathbf{x}' - \mathbf{x}\|_\infty \leq \varepsilon$ to keep the attack imperceptible. In other words, the larger the epsilon, the more perceptible are the perturbations and the more effective are the attacks (meaning classification accuracy deteriorates). It should be noted that FGSM produces adversarial attacks

quickly, but the attacks are not very strong to fool the classifier, as demonstrated by our experiments.

B. Iterative Fast Gradient Sign Method or Basic Iterative Method (BIM)

Iterative FGSM [7] or Basic Iterative Method (BIM) takes iterative smaller steps α in the direction of the gradient in contrast to FGSM which takes a single step

$$\mathbf{x}'_{i+1} = \mathbf{x} + \text{clip}_{\varepsilon}(\mathbf{x}'_i + \alpha \text{sign}(\nabla_{\mathbf{x}'_i} L(g(\mathbf{x}'_i), y^{\text{benign}})) - \mathbf{x}), \quad (2)$$

where $\mathbf{x}'_0 = \mathbf{x}$ and i is iteration step for optimization. The clip function assures that the L_{∞} norm of perturbation is smaller than ε after each optimization step i . This results in a stronger attack than that of FGSM, however it also takes more time to compute. In our experiments, we used $\alpha = \varepsilon/5$.

C. Carlini-Wagner attack

The Carlini-Wagner (CW) attack [6] is computed by finding the minimum perturbation δ that fools the classifier while maintaining imperceptibility. δ is obtained by minimizing the loss,

$$C(\delta) \triangleq D(\mathbf{x}, \mathbf{x} + \delta) + c f(\mathbf{x} + \delta). \quad (3)$$

where, D is a distance metric, typically L_2 norm. By minimizing D , we minimize the perceptibility of the perturbation.

The function f is a criterion defined in such a way that the system fails if and only if $f(\mathbf{x} + \delta) \leq 0$. To perform a non-targeted attack in a classification task, we define $f(\mathbf{x}')$ as,

$$f(\mathbf{x}') = \max(g(\mathbf{x}')_{\text{benign}} - \max\{g(\mathbf{x}')_j, j \neq \text{benign}\} + \kappa, 0) \quad (4)$$

where \mathbf{x}' is the adversarial sample, $g(\mathbf{x}')_j$ is the logit prediction for class j , and κ is a confidence parameter. The attack is successful when $f(\mathbf{x}') \leq 0$. This condition is met when, at least, one of the logits of the non-benign classes is larger than the logits of the benign class plus κ . We can increase the confidence in the attack success by setting $\kappa > 0$.

The weight c balances D and f objectives. The optimization algorithm consists of a nested loop. In the outer loop, A binary search is used to find the optimal c for every utterance. In the inner loop, for each value of c , $C(\delta)$ is optimized by gradient descend iterations. If an attack fails, c is increased in order to increase the weight of the f objective over D , and the optimization is repeated. If the attack is successful, c is reduced.

For our experiments, we set the learning rate parameter as 0.001, confidence κ as 0, the maximum number of inner loop iterations as 10, and the maximum number of halving/doubling of c in the outer loop as 5.

D. Transfer universal attacks

Universal perturbations are adversarial noises that are optimized to be sample-agnostic [56]. Thus, we can add the same universal perturbation to multiple audios and make the classifier to fail for all of them. The algorithm to optimize these universal perturbations is summarized as follows. Given

a set of samples $\mathbf{X} = \{\mathbf{x}_1, \dots, \mathbf{x}_N\}$, we intend to find a perturbation δ , such as $\|\delta\|_{\infty} \leq \varepsilon$, to make it imperceptible, that can fool most samples in \mathbf{X} . The algorithm iterates over the data in \mathbf{X} gradually updating δ . In each iteration i , if the a current perturbation δ doesn't fool sample $\mathbf{x}_i \in \mathbf{X}$, we add an extra perturbation $\Delta\delta_i$ with minimal norm such as the perturbed point $\mathbf{x}_i + \delta + \Delta\delta_i$ fools the classifier. This is done by solving

$$\Delta\delta_i = \arg \min_{\mathbf{r}} \|\mathbf{r}\|_{\infty} \text{ s.t. } g(\mathbf{x}_i + \delta + \mathbf{r}) \neq g(\mathbf{x}_i) \quad (5)$$

where g is the classification network. Then, we enforce the constrain $\|\delta\| \leq \varepsilon$, by projecting the updated perturbation on the ℓ_p ball of radius ε ,

$$\delta \leftarrow \mathcal{P}_{p,\varepsilon}(\delta + \Delta\delta_i) \quad (6)$$

where $\mathcal{P}_{p,\varepsilon}$ is the projection function. We take several iterations over the data in \mathbf{X} to improve the universal perturbation. The iterations stops when at least a proportion P of the samples in \mathbf{X} is miss-classified.

In [56], the authors show that universal perturbation present also cross-model universality. In other words, universal perturbations computed for a specific architecture can also fool other architectures. Hence, it poses a potential security breach to break any classifier. Motivated by this, we used the universal perturbations pre-computed in Armory toolkit¹ to create transfer black-box attacks for our x-vector classifier. These universal perturbations were create using a white-box SincNet classification model [57]².

V. ADVERSARIAL DEFENSES

Defenses against adversarial attacks mainly include adversarial training [58], introducing randomization [59], or using some form of denoising to remove the adversarial perturbation [60]. Adversarial training has proven to be a good defense [48], however, robustness degrades when test-time attacks differ from those used when training the system. Adversarial training significantly increases training time, which hinders scalability when using very large x-vector models. In this work, we focus on preprocessing defenses, which intend to remove the adversarial perturbation from the input signal. These defenses do not have prior knowledge of type and strength of attacks.

A. Randomized smoothing

Randomized smoothing is a method to construct a new *smoothed* classifier g' from a base classifier g . The smoothed classifier g' predicts the class that the base classifier g would predict given an input \mathbf{x} perturbed with isotropic Gaussian noise [59]. That is

$$g'(\mathbf{x}) = \arg \max_c \mathbb{P}(g(\mathbf{x} + \mathbf{n}) = c) \quad (7)$$

$$\mathbf{n} \sim \mathcal{N}(\mathbf{0}, \sigma^2 \mathbf{I}) \quad (8)$$

¹https://github.com/twosixlabs/armory/blob/master/armory/data/adversarial/librispeech_adversarial.py

²<https://github.com/mravaneli/SincNet>

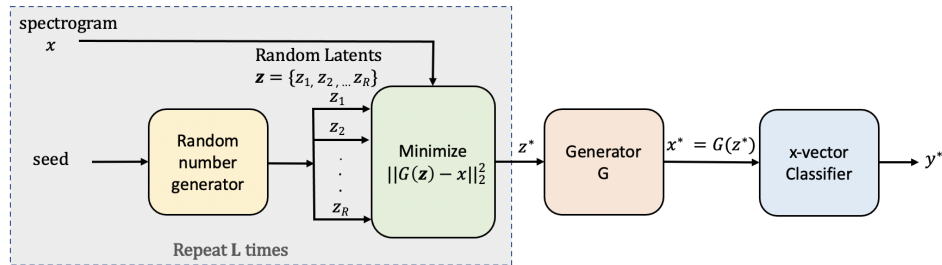


Fig. 2: Scheme of Defense-GAN inference step

where \mathbb{P} is a probability measure and the noise standard deviation σ is an hyperparameter that controls the trade-off between robustness and accuracy. Randomized smoothing is a certifiable defense against attacks with bounded L_2 norm perturbations. In [59], the authors prove tight bounds for certified accuracies under Gaussian noise smoothing. Despite this defense is not certifiable for L_p with $p \neq 2$, we found that it also perform well for other norms like L_∞ .

The main requirement for this defense to be effective is that the base classifier g needs to be robust to Gaussian noise. The base x-vector classifier is already robust to noise since it is trained on speech augmented with real noises [61] and reverberation [62] using a wide range of signal-to-noise ratios and room sizes. However, we robustified our classifier further by adding an extra fine-tuning step. In this step, we fine-tune all the layers of the x-vector classifier by adding Gaussian noise on top of the real noises and reverberations. The training standard deviation was uniformly sampled from the uniform distribution in interval $[0, 0.3]$, assuming a waveform with dynamic range $[-1, 1]$ interval. At test time, we added Gaussian noise with $\sigma = 0.2$. This defense made the system robust for FGSM and BIM (with $L_\infty \leq 0.01$) and CW attacks in comparison to the undefended system. We found that the test σ needed to be significantly larger than the L_∞ norm of the adversarial perturbation for the defense to be effective. We also found that training with random Uniform σ , was better than matching the train and test σ values.

B. Defense-GAN

Generative adversarial networks (GAN) are implicit generative models inspired by game theory [16] where two of two networks, termed Generator G and Discriminator D , compete with each other (hence the name "adversarial"). G maps a low-dimensional latent variable \mathbf{z} to the observed data space \mathbf{x} . The goal of G is to generate samples $G(\mathbf{z})$ that are similar to real data given random variable $\mathbf{z} \sim \mathcal{N}(\mathbf{0}, \mathbf{I})$. Meanwhile, D learns to discriminate between real and generated (fake) samples. D and G are trained alternatively to optimize the following objective

$$V(G, D) = \mathbb{E}_{\mathbf{x} \sim p_{\text{data}}(\mathbf{x})} [\log(D(\mathbf{x}))] + \mathbb{E}_{\mathbf{z} \sim p_z(\mathbf{z})} [\log(1 - D(G(\mathbf{z})))] , \quad (9)$$

which is minimized w.r.t. G and maximized w.r.t. D . When G is being updated, it tries to fool the Discriminator into classifying fake samples as real. When D is being updated, it

learns to detect fake and real samples better. As the training progresses, these adversaries keep improving by learning to fool one other. It can be shown that this objective minimizes the Jensen-Shannon (JS) distance between the real and generated distributions [16].

Wasserstein GAN (WGAN) is an alternative GAN formulation that minimizes the Wasserstein distance rather than the JS distance [63]. Using Kantorovich-Rubinstein duality, the objective that achieves this is

$$V(G, D) = \mathbb{E}_{\mathbf{x} \sim p_{\text{data}}(\mathbf{x})} [D(\mathbf{x})] - \mathbb{E}_{\mathbf{z} \sim p_z(\mathbf{z})} [D(G(\mathbf{z}))] \quad (10)$$

where the network D , termed as *critic*, needs to be a K -Lipschitz function. Wasserstein GAN usually yields better performance than vanilla GAN.

The work in [38] proposes to use GANs as a preprocessing defense against adversarial attacks. This method termed as Defense-GAN has been demonstrated as an effective defense in several computer vision datasets. The key assumptions are that a well-trained generator learns the low dimensional manifold of the clean data, while adversarial samples are outside this manifold. Therefore, projecting the test data onto the manifold defined by the GAN Generator will clean the sample of the adversarial perturbation.

A two-step approach is followed by Defense-GAN. In the training phase, a GAN is trained on benign data to learn the low-dimensional data manifold. In the inference phase, The test sample \mathbf{x} is projected onto the GAN manifold by optimizing latent variable \mathbf{z} to minimize the reconstruction error

$$\mathbf{z}^* = \arg \min_{\mathbf{z}} \|G(\mathbf{z}) - \mathbf{x}\|_2^2 . \quad (11)$$

Then, the projected sample is $\mathbf{x}^* = G(\mathbf{z}^*)$ \mathbf{z} is optimized by L gradient descent iterations, initialized with R random seed (random restarts). Figure 2 outlines the Defense-GAN inference step.

We adapted DefenseGAN to the audio domain. We trained Wasserstein GAN with a Deep Convolutional generator-discriminator (DCGAN) to generate clean log-Mel-Spectrograms, similar to [64]. We enforced the 1-Lipschitz constraint for the Discriminator by adding a gradient penalty loss [65]. The Generator was trained to generate spectrogram patches of 80 frames per each latent variable. At inference, we used the GAN to project adversarial spectrograms to the clean manifold. Note that adversarial perturbation was added in the wave domain, not in the log-spectrogram domain. The DefenseGAN procedure needs to be sequentially

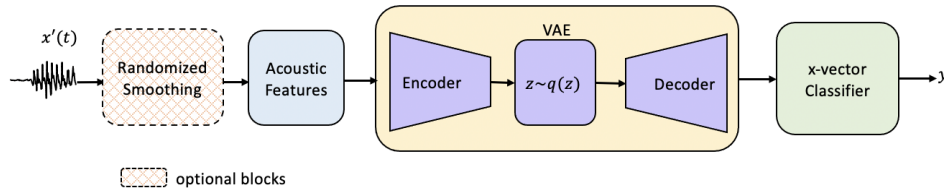


Fig. 3: Pipeline of VAE defense. Combination of VAE with randomized smoothing is indicated by optional block

applied to each block of 80 frames until reconstructing the full utterance spectrogram. We observed that DefenseGAN didn’t achieve high-quality spectrogram generation, which degraded performance on benign samples. To mitigate this, we used a weighted combination of original \mathbf{x} and reconstructed spectrograms \mathbf{x}^* as $\mathbf{x}^{**} = \alpha\mathbf{x}^* + (1 - \alpha)\mathbf{x}$.

The major advantage of Defense-GAN is that it is not trained for any particular type of attack. Therefore, this defense strategy is “attack independent”. Another advantage is that the iterative procedure used for inference is not differentiable. Thus, it is difficult to create adaptive attacks that can break the defense. To perform attacks on this defense, we approximate $\mathbf{x}' \approx \mathbf{x}$ —assuming small adversarial perturbations— for the backward pass. Then the Jacobian of the defense can approximated as an identity matrix. This is termed as *backward pass differentiable approximation* (BPDA) [66].

DefenseGAN has also some disadvantages. The success of Defense-GAN is highly dependent on training a good Generator [38], otherwise, the performance suffers on both original and adversarial examples. Also, it a very slow procedure requiring $R \times L$ forward/backward passes on the Generator. Hyper-parameters L and R need to be tuned to balance speed and accuracy.

C. Variational autoencoder defense

Considering the disadvantages of DefenseGAN, we decided to explore other generative models such as variational auto-encoders (VAE) [67]. Variational auto-encoders are probabilistic latent variable models consisting of two networks, termed encoder and decoder. The decoder defines the generation model of the observed variable \mathbf{x} given the latent \mathbf{z} , i.e., the conditional data likelihood $P(\mathbf{x}|\mathbf{z})$. Meanwhile, the encoder computes the approximate posterior of the latent given the data $q(\mathbf{z}|\mathbf{x})$. The model trained by maximizing the evidence lower bound

$$\mathcal{L} = E_{q(\mathbf{z}|\mathbf{x})} [\log P(\mathbf{x}|\mathbf{z})] - D_{\text{KL}}(q(\mathbf{z}|\mathbf{x})||P(\mathbf{z})) \quad (12)$$

where $P(\mathbf{z})$ is the latent prior, typically standard Normal. The first term of the ELBO intends to minimize the reconstruction loss while the second is a regularization term that keeps the posterior close to the prior. The KL divergence term also helps to create an information bottleneck (IB), limiting the amount of information that flows through the latent variable [68]. We expect that this IB will let pass the most relevant information while removing small adversarial perturbations from the signal.

As for DefenseGAN, we applied this defense in the log-filter-bank domain, as shown in Figure 3. We assumed Gaussian forms for the likelihood and the approximate posterior.

The encoder and decoder predict the means and variances of these distributions. To make our VAE more robust, we trained it on a denoising fashion [69] (Denoising VAE). During training, the latent posterior is compute from a noisy version of the sample, while the decoder tries to predict the original sample. At inference, we compute the latent posterior from the adversarial sample, draw a sample $\mathbf{z} \sim q(\mathbf{z}|\mathbf{x})$; and forward pass \mathbf{z} through the decoder. We used the decoder predicted mean as an estimate of the benign sample. Variational auto-encoders have the advantage that they are easier to train than GANs and inference is also faster, since it just consists of a single forward pass of an encoder/decoder networks. Nevertheless, they have the drawback that they are fully differentiable so and the attacker can adapt to the defense back-propagating gradients through the VAE. In that sense, we considered two alternatives for the defense:

- *Black-box VAE*: The attacker does not know that there is a defense or he/she does not have access to the defense model, so we approximate the Jacobian of the VAE by the identity matrix during back-propagation in the same way as we did with DefenseGAN
- *White-box VAE*: The attacker has full access to the defense model, so we back-propagate gradients to the combined VAE plus x-vector classifier pipeline.

We also experimented with combining Randomized Smoothing and VAE defenses, as illustrated in Figure 3.

D. WaveGAN vocoder defense

The last of the defense that we explored was a WaveGAN vocoder defense. A vocoder reconstructs the speech waveform given a compressed representation of it, in our case log-Mel-Spectrograms. We used the ParallelWaveGAN vocoder proposed in [70]. This vocoder is based on a generative adversarial network similar to DefenseGAN. However, there are some differences

- DefenseGAN reconstructs the clean spectrograms while WaveGAN reconstructs the clean waveform.
- In DefenseGAN, reconstruction is based only on the latent variable \mathbf{z} . Meanwhile in the WaveGAN vocoder, both generator $G(\mathbf{y}, \mathbf{z})$ and discriminator $D(\mathbf{x}, \mathbf{y})$ are also conditioned on the log-Mel Spectrogram \mathbf{y} of the input signal.
- At inference, DefenseGAN needs to iterate to find the optimum value of the latent \mathbf{z} . In the WaveGAN, we just need to forward pass the log-Mel-Spectrogram \mathbf{y} and the latent \mathbf{z} through the WaveGAN generator. \mathbf{z} is a standard Normal random variable with the same length as the input waveform. Figure 4 shows the reconstruction pipeline.

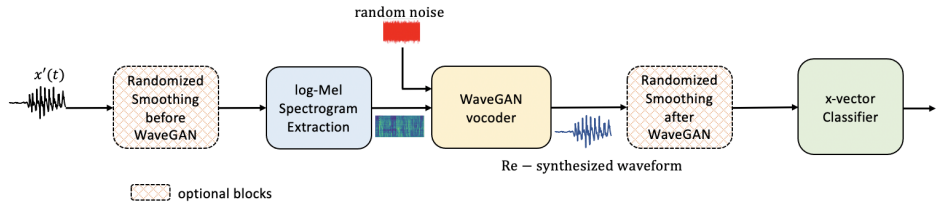


Fig. 4: Pipeline for WaveGAN Vocoder Defense. Combination of WaveGAN with randomized smoothing is indicated by the optional blocks.

This Parallel WaveGAN was trained on a combination of waveform-domain adversarial loss; and a reconstruction loss in Short Time Fourier Transform (STFT) domain. The reconstruction loss improves the stability and efficiency of the adversarial training. It is the sum of several STFT losses computed with different spectral analysis parameters (window length/shift, FFT length). ParallelWaveGAN training scheme combines adversarial and multi-resolution STFT losses. The architecture of the generator is a non-autoregressive WaveNet, while the architecture for the Discriminator is based on a dilated convolutional network.

We considered two alternatives regarding the knowledge of the attacker. *Black-box WaveGAN* where the attacker does not have access to the WaveGAN model; and *White-box WaveGAN* where the attacker can use the WaveGAN model to adapt the attack to the defense.

As shown by the optional blocks in Figure 4, we can also combine smoothing and WaveGAN defenses. Here, we can choose whether we want to apply smoothing before or after the WaveGAN.

VI. EXPERIMENTAL SETUP

A. Dataset and task

The DARPA program *Guaranteeing AI Robustness Against Deception* (GARD)³ promotes research on defenses against adversarial attacks in different domains. The program organizes periodic evaluations to benchmark the defenses developed by the participants. Our experimental setup is based on the most recent GARD evaluation on defenses for speaker identification systems. The proposed task is closed-set speaker identification, also known as speaker classification. Given a test utterance, the task is to identify the most likely among the enrolled speakers.

The speaker identification task is built on the LibriSpeech dataset [71] development set, which contains 40 speakers (20 male and 20 female). The development set was split into training (GARD-train), validation (GARD-val), and test (GARD-test). Each speaker has about 4 minutes for enrollment and 2 minutes for test, with a total of 1283 test recordings. While the setup is small, we need to take into account the extensive computing cost of performing adversarial attacks. For example, Carlini-Wagner attacks require hundreds of gradient descent iterations to obtain the adversarial perturbation. Also, note that following Doddington’s rule of 30 [72], with 1283 recordings, we can measure error rates as low as 2.3% with confidence (97.7% accuracy). Thus, the dataset was selected

to be able to obtain meaningful conclusions while limiting computing cost.

We will compare the performance of attacks and defenses using classification accuracy as the primary metric. Attacks will degrade the accuracy while defenses will try to increase accuracy to match one of the non-attacked systems. To quantify the strength of the attack, we will indicate the L_∞ norm of the adversarial perturbation, assuming that the waveform’s dynamic range is normalized to $[-1, 1]$.

This experimental setup is publicly available through the Armory toolkit⁴. Armory toolkit uses the attacks available in the Adversarial Robustness Toolbox⁵ to generate the adversarial samples.

B. Baseline

We experimented with different x-vector architectures for our undefended baseline. Adversarial perturbations were added in the wave domain. Acoustic features were 80 dimension log-Mel-filter-banks with short-time mean normalization. These features are used as input to x-vector networks based on ThinResNet34, ResNet34, EfficientNet-b0/b4 or Transformer-Encoder as described in Section II. The network predicts logits for the speaker classes. The full pipeline was implemented in PyTorch [73] so we can back-propagate gradients from the final score to the waveform. Note that we used state-of-the-art architectures. They provided equal error rates between 1.17% (ResNet34) to 1.9% (ThinResNet34) on the popular VoxCeleb1 test set. We observed that all the architectures are extremely vulnerable to attacks. EfficientNet x-vector was more robust overall but had a higher computing cost than other architectures. For this reason, we decided to evaluate our defenses on ThinResNet34, which allowed us to perform experiments faster.

The x-vector networks were pre-trained on the VoxCeleb2 dataset [74], comprising 6114 speakers. Training data was augmented 6× with noise from the MUSAN corpus⁶ and impulse responses from the RIR dataset⁷. We used additive angular margin softmax loss (AAM-Softmax) [51] with margin=0.3 and scale=30 and Adam optimizer to train the network. To use this network for speaker identification on the LibriSpeech dev set, we restarted the last two layers of the network and fine-tuned on the LibriSpeech dev train partition. We fine-tuned with AAM-Softmax with margin=0.9, since increasing the margin slightly improved performance in this set.

⁴<https://github.com/twosixlabs/armory/blob/master/docs/scenarios.md>

⁵<https://github.com/Trusted-AI/adversarial-robustness-toolbox>

⁶<http://www.openslr.org/resources/17>

⁷<http://www.openslr.org/resources/28>

³<https://www.darpa.mil/program/guaranteeing-ai-robustness-against-deception>

TABLE II: GAN generator/discriminator architectures. For generator, latent_dim =100 and ReLU activations were used after each deconvolution layer. For Discriminator, LeakyReLU activations with negative slope = 0.2 were used after each convolution layer. For both, the output padding is 1×1

Generator		
Layer name	Structure	Output
Input	-	latent_dim
Linear	-	16384
Reshape	-	$1024 \times 4 \times 4$
ConvTranspose2d-1	3×3 , 1024, Stride 3	$512 \times 7 \times 7$
ConvTranspose2d-2	3×3 , 512, Stride 3	$256 \times 13 \times 13$
ConvTranspose2d-3	3×3 , 256, Stride 3	$128 \times 25 \times 25$
ConvTranspose2d-4	3×3 , 128, Stride 3	$64 \times 49 \times 49$
ConvTranspose2d-5	3×3 , 64, Stride 3	$1 \times 97 \times 97$
Crop center	-	$1 \times 80 \times 80$
Discriminator		
Layer name	Structure	Output
Input	-	$1 \times 80 \times 80$
Conv2d-1	3×3 , 64, Stride 2	$64 \times 40 \times 40$
Conv2d-2	3×3 , 128, Stride 2	$128 \times 20 \times 20$
Conv2d-3	3×3 , 256, Stride 2	$256 \times 10 \times 10$
Conv2d-4	5×5 , 512, Stride 2	$512 \times 4 \times 4$
Conv2d-5	5×5 , 1024, Stride 2	$1024 \times 1 \times 1$
Reshape	-	1024
Linear	-	1

C. Adversarial Attacks

We experimented with attacks implemented in the Adversarial Robustness Toolkit: fast gradient sign method (FGSM), basic iterative method (BIM) (a.k.a. IterFGSM), Carlini-Wagner-L2, and Universal Perturbations. For FGSM and BIM, we tested L_∞ norms ε between 0.0001 and 0.2. For BIM, we used a learning rate $\alpha = \varepsilon/5$, and performed seven iterations. For Carlini-Wagner, we used confidence $\kappa = 0$, learning rate 0.001, 10 iterations in the inner loop, and a maximum of 10 iterations in the outer loop. Universal perturbations were transferred from a SincNet model [57], to create transfer black-box attacks as explained in Section IV-D.

D. Defenses

1) *Randomized smoothing defense*: To improve the performance for the randomized smoothing defense, we fine-tuned the network with Gaussian noise with $\sigma \sim \mathcal{U}(0.0.3)$ on top of real noises and reverberation. We compared three versions: fine-tuning the network classification head (last two layers) without Gaussian noise; fine-tuning the head network with Gaussian Noise, and fine-tuning the full network with Gaussian noise. At inference time, we experimented by using one or multiple smoothed samples. When using multiple samples, we add several noise signals to the utterance, evaluate each one of them and average the outputs.

2) *Defense-GAN*: The GAN in DefenseGAN used a Deep Convolutional generator-discriminator (DCGAN) trained with Wasserstein and gradient penalty losses, similar to [64]. It was trained on VoxCeleb2 using the same log-Mel-filter-bank features required by the x-vector networks. The generator and discriminator architectures are shown in Table II. The generator projects the latent variable \mathbf{z} with dimension 100 to $256 \times d$ dimension and reshape to create a tensor of size 16×16 with $16 \times d$ channels. A sequence of $2D$

transposed convolutions with stride 2 upsamples this tensor to generate square log-Mel-filter-bank patches with 80 frames of dimension 80. The critic is a sequence of $2D$ convolutions with stride 2, which downsample the input to generate a single output per filter-bank patch. We did not observe improvements by increasing the complexity of generator and discriminator networks. At inference time, the DefenseGAN procedure used 0.025 learning rate, 300 iterations, and 10 random seeds.

3) *Variational auto-encoder defense*: A denoising VAE was trained on VoxCeleb2 augmented with noise and reverberation to model the manifold of benign log-Mel-Spectrograms. Contrary to DefenseGAN, the VAE improved the reconstruction error when increasing the complexity of the encoder/decoder architectures. The architectures that performed the best were based on 2D residual networks. Table III describes the Encoder/Decoder architectures. The encoder downsamples the input spectrogram in time and frequency dimension multiple times to create an information bottleneck. The output of the encoder is the mean of the posterior $q(\mathbf{z}|\mathbf{x})$, while the variance is kept as trainable constant. Meanwhile, the decoder is a mirrored version of the encoder. It takes the latent sample $\mathbf{z} \sim q(\mathbf{z}|\mathbf{x})$ and upsamples it to predict the mean of $P(\mathbf{x}|\mathbf{z})$. The variance is also a trainable constant. To perform the upsampling operation, we used subpixel convolutions, since they provide better quality than transposed convolutions [75].

4) *WaveGAN vocoder defense*: For the ParallelWaveGAN vocoder, we used the implementation available in ⁸. We compared two models trained on different datasets. First, the public model trained on the Artic Voices [76] datasets. Second, we trained a model on VoxCeleb2 [77].

VII. RESULTS

A. Undefended baselines

We compared the vulnerability of ResNet34, EfficientNet, Transformer and ThinResNet34 x-vector to adversarial attacks. Table IV shows classification accuracy for undefended baselines under FGSM, BIM, CW, and universal transfer attacks. The systems are robust to the Universal transfer attack obtaining accuracy similar to the clean condition. This indicates that the attacker cannot transfer attacks from white-box models that are very different from the victim model verifying the claim by [31].

For FGSM attacks, we only observed strong degradation for $L_\infty \geq 0.1$. However, for iterative attacks (BIM, CW), all systems failed even with imperceptible perturbations. The system using a fusion of the above networks gives light improvements (especially for BIM attacks with $L_\infty \leq 0.1$ and CW); however, the system is still vulnerable. In the following sections, we analyze the defenses using the ThinResNet34 x-vector. This is mainly motivated by the high computing cost of performing adversarial attacks. Note that ThinResNet34 is around $16 \times$ faster than the full ResNet34 architecture.

B. Randomized smoothing defense

Table V shows the results for the randomized smoothing defense. We experimented with different Gaussian noise stan-

⁸<https://github.com/kan-bayashi/ParallelWaveGAN>

TABLE III: ResNet2d VAE encoder/decoder architectures. The first dimension of the input shows number of filter-banks, and the third dimension indicates the number of frames T . Batchnorm and ReLU activations were used after each convolution. Subpixel convolutions were used for upsampling operations.

Layer name	Encoder		Decoder	
	Structure	Output	Structure	Output
Input	–	$80 \times 1 \times T$	–	$10 \times 80 \times T/8$
Conv2D-1	$5 \times 5, 64, \text{Stride } 1$	$80 \times 64 \times T$	$3 \times 3, 512, \text{Stride } 1$	$10 \times 512 \times T/8$
ResNetBlock-1	$\begin{bmatrix} 3 \times 3, 64 \\ 3 \times 3, 64 \end{bmatrix} \times 2, \text{Stride } 1$	$80 \times 64 \times T$	$\begin{bmatrix} 3 \times 3, 512 \\ 3 \times 3, 512 \end{bmatrix} \times 2, \text{Stride } 1$	$10 \times 512 \times T/8$
ResNetBlock-2	$\begin{bmatrix} 3 \times 3, 128 \\ 3 \times 3, 128 \end{bmatrix} \times 2, \text{Stride } 2$	$40 \times 128 \times T/2$	$\begin{bmatrix} 3 \times 3, 256 \\ 3 \times 3, 256 \end{bmatrix} \times 2, \text{Stride } 2$	$20 \times 256 \times T/4$
ResNetBlock-3	$\begin{bmatrix} 3 \times 3, 256 \\ 3 \times 3, 256 \end{bmatrix} \times 2, \text{Stride } 2$	$20 \times 256 \times T/4$	$\begin{bmatrix} 3 \times 3, 128 \\ 3 \times 3, 128 \end{bmatrix} \times 2, \text{Stride } 2$	$40 \times 128 \times T/2$
ResNetBlock-4	$\begin{bmatrix} 3 \times 3, 512 \\ 3 \times 3, 512 \end{bmatrix} \times 2, \text{Stride } 2$	$10 \times 512 \times T/8$	$\begin{bmatrix} 3 \times 3, 64 \\ 3 \times 3, 64 \end{bmatrix} \times 2, \text{Stride } 2$	$80 \times 64 \times T$
Projection	$1 \times 1, 80, \text{Stride } 1$	$10 \times 80 \times T/8$	$1 \times 1, 1, \text{Stride } 1$	$80 \times 1 \times T$

TABLE IV: Classification accuracy (%) for several undefended x-vector architectures under adversarial attacks

Architecture	Clean	FGSM Attack					BIM Attack					Universal	CW
L_∞		0.0001	0.001	0.01	0.1	0.2	0.0001	0.001	0.01	0.1	0.2	0.3	-
1. ResNet34	100.0	99.1	95.8	95.6	93.3	87.2	92.2	14.8	0.0	0.0	0.0	100.0	1.3
2. EfficientNet-b0	100.0	99.2	95.6	93.0	93.6	88.1	96.9	27.7	0.0	0.0	0.0	100.0	0.8
3. EfficientNet-b4	100.0	99.5	95.8	92.3	93.1	88.8	98.1	30.5	0.0	0.0	0.0	100.0	0.0
4. Transformer	99.5	96.3	80.6	76.4	49.5	32.1	81.9	20.3	0.2	0.0	0.0	99.9	1.9
5. ThinResNet34	100.0	98.0	91.1	89.2	85.6	74.5	88.0	2.2	0.0	0.0	0.0	100.0	1.1
Fusion 2+4+5	100.0	99.8	97.5	97.0	88.4	78.0	98.9	66.4	16.1	0.0	0.2	100.0	49.1

TABLE V: Classification accuracy (%) for randomized smoothing defense. We compare fine-tuning x-vector w/o Gaussian noise; and finetuning the network clasification head versus the full network.

Gaussian Augment	Smoothing σ	Clean	FGSM Attack					BIM Attack					Universal	CW	
L_∞			0.0001	0.001	0.01	0.1	0.2	0.0001	0.001	0.01	0.1	0.2	0.3	-	
No	0	100.0	98.0	91.1	89.2	85.6	74.5	88.0	2.2	0.0	0.0	0.0	100.0	1.1	
	0.01	100.0	100.0	100.0	67.8	71.6	64.1	99.8	99.4	0.0	0.2	0.0	99.9	7.5	
	0.1	98.0	98.0	97.5	94.4	26.4	25.8	97.8	97.5	90.3	2.5	2.2	98.7	83.4	
	0.2		87.3	88.8	87.3	85.8	30.2	19.5	86.4	85.3	82.2	9.5	6.7	90.3	87.3
Yes Head	0	100.0	96.9	90.0	92.3	93.4	91.1	83.4	2.3	0.0	0.0	0.0	100.0	1.4	
	0.01	100.0	100.0	99.2	78.8	83.1	81.6	100.0	99.1	0.6	0.0	0.0	100.0	8.8	
	0.1	98.6	98.6	98.9	97.8	47.3	45.3	99.2	98.6	97.3	0.9	1.1	99.5	81.6	
	0.2		97.0	97.5	96.7	96.7	51.9	35.8	97.7	97.2	95.8	7.5	1.7	98.5	95.3
Yes Full-Net	0	99.4	97.0	90.5	94.5	94.8	90.6	88.0	17.2	0.5	0.5	0.3	99.9	2.0	
	0.2	98.0	98.3	98.4	97.0	64.4	44.1	97.2	97.8	97.7	18.9	2.0	98.7	96.9	
	0.4	92.5	92.2	94.5	93.1	65.3	40.9	93.1	93.1	91.9	44.8	9.5	95.3	93.1	

dard deviations σ . Unless indicated otherwise, we use a single noisy sample for the randomized smoothing.

The first block of the table shows results for ThinResNet34 fine-tuned without Gaussian noise (only real noise and reverberation). Smoothing only damages clean and universal attack performance when using very high $\sigma = 0.2$, which is very perceptible noise. We also observe that smoothing damaged accuracy under FGSM attacks as we increase the smoothing σ . However, it improves accuracy under BIM and CW attacks. To make the system robust to BIM attacks, we needed $\sigma \sim 10 \times L_\infty$. It also provided a huge improvement for the Carlini-Wagner attack w.r.t. the undefended system.

In the second block, we fine-tuned the network head with Gaussian noise on top of real noise and reverberation. By doing this, we increased the robustness of the system for the

smoothing defense. Thus, the performance for clean and universal with high smoothing σ was improved, being close to the performance without defense. It also significantly improved the accuracy under FGSM with $L_\infty \in [0.01, 0.2]$ —in some cases up to 100% of relative improvement w.r.t the system fine-tuned without Gaussian noise. It also improved BIM at $L_\infty = 0.01$. When using multiple smoothing samples—denoted as 0.1×10 , accuracy degraded. This was because averaging multiple noise samples provides a better estimation of the gradients for the attacker.

In the third block, we fine-tuned the full x-vector network with Gaussian noise. This allowed us to obtain good accuracies for very high smoothing $\sigma \in [0.2, 0.4]$. In most attacks, we got similar or better results than when fine-tuning just the head. For $\sigma = 0.2$, we obtained the best results overall. For $\sigma = 0.4$,

we achieved the best results under BIM attack with $L_\infty \geq 0.1$, at the cost of damaging accuracy in low L_∞ attacks.

C. Defense GAN

We observed that the DefenseGAN generated spectrograms are losing minute details and degraded benign signal performance. As explained in Section V-B, we interpolated the original and reconstructed spectrograms using a factor α . We selected $\alpha = 0.5$ to maintain high benign accuracy at the same time that we improve robustness against BIM and CW attacks. Lower $\alpha = 0.25$, provided better benign accuracy, but no improved w.r.t. the undefended systems. Higher $\alpha = 0.75$, degraded benign accuracy down to 72%. Table VI compares DefenseGAN versus undefended classification accuracies. DefenseGAN degraded FGSM attacks but improved BIM and CW attacks. For CW, we get an accuracy of 60.94% against 1.41% without defense. This shows that DefenseGAN has good potential to defend against CW attack. This finding is similar to DefenseGAN for CW attack on images [38].

D. Variational Auto-encoder (VAE) defense

Table VII presents the VAE defense results. First, we use VAE as a pre-processing defense for the original ThinRes-Net34 x-vector (*No fine-tuning* block in the table). We compare the case where the attacker does not have access to the VAE model (Black-box VAE) versus the case where the attacker knows the VAE model and can back-propagate through it (White-box VAE). Black-box VAE degrades FGSM w.r.t. undefended for high $L_\infty > 0.01$, which are perceptible. However, it provides significant improvements for BIM $L_\infty \leq 0.01$ —2.3% to 71.4% for $L_\infty = 0.01$ — and Carlini-Wagner—1.4% to 71.1%. When using White-Box VAE, adversarial accuracies reduced. We only observe significant improvements w.r.t. undefended for BIM $L_\infty = 0.01$ and Carlini-Wagner.

Introducing VAE degraded clean accuracy about 10% absolute. To counteract this, we fine-tuned the x-vector model, including the VAE in the pipeline. Fine-tuning improved clean, FGSM, and universal transfer attack accuracies, being close to the ones of the undefended system. Again, VAE improved BIM, and CW attacks w.r.t. the undefended system.

Finally, we combined VAE and randomized smoothing defenses. Smoothing $\sigma = 0.2$ plus Black-box VAE improved all BIM and CW attacks with respect to just VAE. It also improved w.r.t. just smoothing $\sigma = 0.2$ in Table V. Only BIM with $L_\infty = 0.2$, which is very perceptible, was seriously degraded w.r.t. to the clean condition. For the case of Smoothing + White-Box VAE, BIM and CW also improved with respect to just White-box VAE. However, there was no significant improvement w.r.t. just smoothing.

E. WaveGAN vocoder defense

Table VIII displays the WaveGAN defense results. We start using WaveGAN as a black-box block from the attacker point of view and compare the publicly available model trained on Artic to our model trained on the VoxCeleb test set. We observe that the VoxCeleb model performed better in the benign condition and across all attacks. We conclude that the larger

variability in terms of speakers and channels in VoxCeleb contributes to making the defense more robust. Contrary to the VAE experiments above, WaveGAN did not degrade the benign accuracy. Thus, we did not need to fine-tune the x-vector network, including the WaveGAN in the pipeline. The black-box VoxCeleb WaveGAN provided very high adversarial robustness with accuracies $> 90\%$ for most attacks. The average absolute improvement overall attacks was 41.5% w.r.t. the baseline. The improvement for BIM (80.47% absolute) and CW (97.34% absolute) is noteworthy. This is very superior to previous smoothing and VAE defenses. However, white-box WaveGAN performance degraded significantly w.r.t. black-box. In the white-box setting, WaveGAN only improved in BIM $L_\infty < 0.01$ and CW, similarly to white-box VAE.

We tried to improve further by integrating smoothing with the WaveGAN vocoder Defense. We can do it in two ways: applying smoothing before or after the vocoder. The results are shown in the third and fourth blocks of Table VIII. We did not observe significant statistical differences between both variants for smoothing $\sigma < 0.1$. For $\sigma \geq 0.1$, smoothing followed by WaveGAN was better. However, overall, adding smoothing to the black-box WaveGAN did not provide consistent improvements w.r.t. just the WaveGAN.

The last line of the table shows the results for smoothing followed by the white-box WaveGAN. In this case, accuracy was similar to the case of just using smoothing. We conclude that combining smoothing and WaveGAN vocoder defense is the best strategy. When the attacker does not have access to the defense model, it is robust across attacks and L_∞ levels. When the attacker can back-propagate through the WaveGAN, it still maintains competitive robustness for most attacks, except those with very high L_∞ norms.

VIII. CONCLUSION

We studied the robustness of several x-vector speaker identification systems to adversarial attacks, and analyzed four defenses to increase adversarial robustness. Table IX summarizes the results for the best configurations of each defense. The proposed defenses degraded benign accuracies very little—4.8% absolute in the worse case. This is a very mild degradation compared to the robustness when the system is adversarially attacked. We observed that undefended systems were inherently robust to FGSM and Black-box Universal attacks transferred from a speaker identification system with different architecture. However, they were extremely vulnerable under Iterative FGSM and Carlini-Wagner attacks.

The simple randomized smoothing defense robustified the system for imperceptible BIM ($L_\infty \leq 0.01$) and Carlini-Wagner recovering classification accuracies $\sim 97\%$. We also explored defenses based on three types of generative models: DefenseGAN, VAE, and WaveGAN vocoder. These models learn the manifold of benign samples and were used to project adversarial examples (outside of the manifold) back into the clean manifold. DefenseGAN and VAE worked at the log-spectrogram level, while WaveGAN worked at the waveform level. We noted that DefenseGAN performed poorly. For VAE and WaveGAN we considered two configurations: attacker

TABLE VI: Classification accuracy (%) for DefenseGAN defense with $\alpha = 0.25$ and $\alpha = 0.5$

DefenseGAN	Clean	FGSM Attack					BIM Attack					Universal	CW
L_∞		0.0001	0.001	0.01	0.1	0.2	0.0001	0.001	0.01	0.1	0.2	0.3	-
No Defense	100.0	96.9	90.0	92.3	93.4	91.1	83.4	2.3	0.0	0.0	0.0	100.0	1.4
$\alpha = 0.5$	95.9	91.6	84.2	81.9	49.4	23.3	85.0	23.6	2.8	1.4	1.6	96.9	60.9

TABLE VII: Classification accuracy (%) for VAE Defense with and without randomized smoothing; with and without fine-tuning the x-vector classifier with the VAE pre-processing; considering VAE as a black-box or white-box block for the attacker.

x-Vector fine-tuning	Smooth σ	VAE Type	Clean	FGSM Attack					BIM Attack					Universal	CW
L_∞				0.0001	0.001	0.01	0.1	0.2	0.0001	0.001	0.01	0.1	0.2	0.3	-
No defense	-	-	100.0	96.9	90.0	92.3	93.4	91.1	83.4	2.3	0.0	0.0	0.0	100.0	1.4
No	0.0	Blackbox	90.8	91.6	88.8	77.8	51.4	44.1	89.4	71.4	34.2	4.4	2.5	91.8	71.1
	0.0	Whitebox	91.6	86.6	75.5	63.8	45.3	38.4	78.8	22.3	4.1	1.9	0.9	91.8	52.5
Yes	0.0	Blackbox	98.9	98.4	98.1	94.2	91.4	84.8	94.7	67.2	12.7	0.9	1.1	99.9	56.1
	0.1	Blackbox	96.9	96.9	97.0	96.9	75.2	57.5	96.9	97.5	96.6	25.6	1.4	98.7	98.0
	0.2	Blackbox	95.2	95.8	95.5	94.7	79.5	51.4	96.6	95.2	94.5	63.1	9.8	97.5	95.5
	0.0	Whitebox	99.4	96.9	94.1	94.2	91.4	84.8	92.3	35.3	1.3	0.9	0.5	99.8	50.2
	0.1	Whitebox	96.6	97.0	96.4	95.8	64.5	53.3	97.5	97.8	94.7	2.2	0.9	98.5	96.9
	0.2	Whitebox	95.2	95.8	96.1	95.2	65.6	50.0	96.1	95.8	94.2	19.1	2.7	97.4	95.8

TABLE VIII: Classification accuracy (%) for WaveGAN defense with and without randomized smoothing; considering WaveGAN as a black-box or white-box block for the attacker. WaveGAN was trained on VoxCeleb, except the pretrained model, which was trained on Artic.

Defense	Smooth σ	Clean	FGSM Attack					BIM Attack					Universal	CW
L_∞			0.0001	0.001	0.01	0.1	0.2	0.0001	0.001	0.01	0.1	0.2	0.3	-
No defense	-	100.0	96.9	90.0	92.3	93.4	91.1	83.4	2.3	0.0	0.0	0.0	100.0	1.4
Pretrained-Black-box	0	96.4	97.3	97.8	90.3	33.9	12.7	96.6	98.3	93.8	64.4	36.3	97.6	95.8
Black-box	0	99.5	99.5	99.7	99.1	86.6	77.2	99.4	99.7	99.5	97.2	92.3	99.9	98.8
Whitebox	0	97.0	98.8	95.8	93.6	83.0	62.3	94.7	36.4	0.8	0.8	0.8	99.8	37.5
Black-box WaveGAN + Smoothing	0.0	99.5	99.7	99.8	98.6	89.7	76.7	99.4	99.5	99.5	97.3	92.5	99.8	99.7
	0.001	99.7	99.5	99.7	99.2	85.0	71.7	99.7	99.7	99.4	97.0	92.3	99.9	99.5
	0.01	99.6	99.4	99.5	99.7	87.5	64.8	99.5	99.7	99.7	97.2	92.7	99.9	99.5
	0.1	97.1	97.3	97.2	96.4	89.1	65.3	97.3	97.0	96.4	95.8	90.5	98.6	97.0
Smoothing + Black-box WaveGAN	0.0	99.5	99.5	99.7	99.1	86.6	77.2	99.4	99.7	99.5	97.2	92.3	99.9	98.8
	0.001	99.7	99.7	99.7	99.2	86.3	69.1	99.7	99.7	99.5	97.2	90.5	99.9	99.2
	0.01	99.6	99.4	99.5	99.4	88.1	65.5	99.5	99.5	99.5	96.4	91.4	99.9	98.8
	0.1	97.1	97.5	98.1	98.4	94.2	76.6	98.4	98.8	98.0	97.0	93.1	99.3	97.3
+ White-box WaveGAN	0.2	95.6	95.2	96.3	95.8	93.0	74.2	94.8	94.8	96.9	95.5	93.4	97.5	95.2
	0.2	95.8	94.7	95.6	94.4	88.9	60.6	95.2	93.3	86.7	14.4	3.1	97.4	92.8

having knowledge of the defense (white-box) or not (black-box). In the black-box setting, both VAE and WaveGAN significantly improved adversarial robustness w.r.t. undefended system. WaveGAN performed the best, being close to the clean condition. For BIM attacks, WaveGAN improved average accuracy from 17.16% to a staggering 97.63%. For CW, it improved from 1.4% to 98.8%. However, in the white-box setting, VAE and WaveGAN protection dropped significantly—WaveGAN accuracy dropped to 37% for CW attack.

Finally, we experimented with combining randomized smoothing with VAE or WaveGAN. We found that smoothing followed by WaveGAN vocoder is the most effective defense. In the black-box setting, it protected against all attacks, includ-

ing perceptible attacks with high L_∞ perturbations—average accuracy was 93% compared to 52% in the undefended system. In the white-box setting, accuracy only degraded for perceptible perturbations with $L_\infty > 0.01$.

In the future, we plan to evaluate these defenses in other speech tasks like automatic speech recognition tasks. Also, we plan to study how to improve the robustness of generative pre-processing defenses in the white-box setting.

REFERENCES

[1] R. K. Das, X. Tian, T. Kinnunen, and H. Li, “The Attacker’s Perspective on Automatic Speaker Verification: An Overview,” *arXiv:2004.08849 [cs, eess]*, Apr. 2020, arXiv: 2004.08849. [Online]. Available: <http://arxiv.org/abs/2004.08849>

TABLE IX: Summary of classification accuracy (%) of all defenses with their best setting. Note: Smoothing $\sigma = 0.2$, WaveGAN models is trained on Voxceleb, and smoothing is applied before WaveGAN/VAE.

Defense	Clean	FGSM Attack					BIM Attack					Universal	CW
		0.0001	0.001	0.01	0.1	0.2	0.0001	0.001	0.01	0.1	0.2		
L_∞	-	0.0001	0.001	0.01	0.1	0.2	0.0001	0.001	0.01	0.1	0.2	0.3	-
No defense	100.0	96.9	90.0	92.3	93.4	91.1	83.4	2.3	0.0	0.0	0.0	100.0	1.4
Smoothing	98.0	98.3	98.4	97.0	64.4	44.1	97.2	97.8	97.7	18.9	2.0	98.7	96.9
DefenseGAN	96.3	91.6	84.2	81.9	49.4	23.3	85.0	23.6	2.8	1.4	1.6	96.9	60.9
VAE-blackbox	98.9	98.4	98.1	94.2	91.4	84.8	94.7	67.2	12.7	0.9	1.1	99.9	56.1
VAE-whitebox	99.4	96.9	94.1	94.2	91.4	84.8	92.3	35.3	1.3	0.9	0.5	99.8	50.2
Smoothing+VAE-blackbox	95.2	95.8	95.5	94.7	79.5	51.4	96.6	95.2	94.5	63.1	9.8	97.5	95.5
Smoothing+VAE-whitebox	95.2	95.8	96.1	95.2	65.6	50.0	96.1	95.8	94.2	19.1	2.7	97.4	95.8
WaveGAN-blackbox	99.5	99.5	99.7	99.1	86.6	77.2	99.4	99.7	99.5	97.2	92.3	99.9	98.8
WaveGAN-whitebox	97.0	98.8	95.8	93.6	83.0	62.3	94.7	36.4	0.8	0.8	0.8	99.8	37.5
Smoothing+WaveGAN-blackbox	95.6	95.2	96.3	95.8	93.0	74.2	94.8	94.8	96.9	95.5	93.4	97.5	95.2
Smoothing+WaveGAN-whitebox	95.8	94.7	95.6	94.4	88.9	60.6	95.2	93.3	86.7	14.4	3.1	97.4	92.8

- [2] M. Todisco, X. Wang, V. Vestman, M. Sahidullah, H. Delgado, A. Nautsch, J. Yamagishi, N. Evans, T. Kinnunen, and K. A. Lee, "ASVSpooF 2019: Future horizons in spoofed and fake audio detection," in *INTERSPEECH 2019*, Graz, Austria, sep 2019, pp. 1008–1012.
- [3] C.-I. Lai, N. Chen, J. Villalba, and N. Dehak, "ASSERT: Anti-Spoofing with Squeeze-Excitation and Residual neTworks," in *INTERSPEECH 2019*, Graz, Austria, sep 2019.
- [4] C. Szegedy, W. Zaremba, I. Sutskever, J. Bruna, D. Erhan, I. J. Goodfellow, and R. Fergus, "Intriguing properties of neural networks," in *ICLR 2014*, 2014.
- [5] I. J. Goodfellow, J. Shlens, and C. Szegedy, "Explaining and Harnessing Adversarial Examples," in *ICLR 2015*, dec 2015.
- [6] N. Carlini and D. Wagner, "Towards Evaluating the Robustness of Neural Networks," in *IEEE Symposium on Security and Privacy, 2017*, aug 2016.
- [7] A. Kurakin, I. J. Goodfellow, and S. Bengio, "Adversarial examples in the physical world," in *CoRR 2017*, jul 2017.
- [8] Y. Dong, Q.-A. Fu, X. Yang, T. Pang, H. Su, Z. Xiao, and J. Zhu, "Benchmarking Adversarial Robustness," dec 2019.
- [9] H. X. Y. M. Hao-Chen, L. D. Deb, H. L. J.-L. T. Anil, and K. Jain, "Adversarial attacks and defenses in images, graphs and text: A review," *International Journal of Automation and Computing*, vol. 17, no. 2, pp. 151–178, 2020.
- [10] D. Amodei, S. Ananthanarayanan, R. Anubhai, J. Bai, E. Battenberg, C. Case, J. Casper, B. Catanzaro, Q. Cheng, G. Chen *et al.*, "Deep speech 2: End-to-end speech recognition in english and mandarin," in *International conference on machine learning*, 2016, pp. 173–182.
- [11] M. Cisse, Y. Adi, N. Neverova, and J. Keshet, "Houdini: Fooling Deep Structured Prediction Models," in *NIPS 2017*, jul 2017, pp. 6977–6987.
- [12] N. Carlini and D. Wagner, "Audio adversarial examples: Targeted attacks on speech-to-text," in *SPW 2018*, 2018.
- [13] P. Neekhara, S. Hussain, P. Pandey, S. Dubnov, J. McAuley, and F. Koushanfar, "Universal Adversarial Perturbations for Speech Recognition Systems," in *INTERSPEECH 2019*, Graz, Austria, sep 2019, pp. 481–485.
- [14] D. Iyer, J. Huang, and M. Jermann, "Generating adversarial examples for speech recognition," Tech. Rep., 2017.
- [15] A. van den Oord, S. Dieleman, H. Zen, K. Simonyan, O. Vinyals, A. Graves, N. Kalchbrenner, A. Senior, and K. Kavukcuoglu, "Wavenet: A generative model for raw audio," 2016.
- [16] I. J. Goodfellow, J. Pouget-Abadie, M. Mirza, B. Xu, D. Warde-Farley, S. Ozair, A. Courville, and Y. Bengio, "Generative Adversarial Networks," *arXiv:1406.2661 [cs, stat]*, Jun. 2014, arXiv: 1406.2661. [Online]. Available: <http://arxiv.org/abs/1406.2661>
- [17] D. Povey, A. Ghoshal, G. Boulianne, L. Burget, O. Glembek, N. Goel, M. Hannemann, P. Motlicek, Y. Qian, P. Schwarz *et al.*, "The kaldi speech recognition toolkit," in *IEEE 2011 workshop on automatic speech recognition and understanding*, no. CONF. IEEE Signal Processing Society, 2011.
- [18] X. Yuan, Y. Chen, Y. Zhao, Y. Long, X. Liu, K. Chen, S. Zhang, H. Huang, X. Wang, and C. A. Gunter, "CommanderSong: A Systematic Approach for Practical Adversarial Voice Recognition," in *USENIX Security 2018*, jan 2018.
- [19] L. Schonherr, K. Kohls, S. Zeiler, T. Holz, and D. Kolossa, "Adversarial Attacks Against Automatic Speech Recognition Systems via Psychoacoustic Hiding," in *NDSS 2019*, Reston, VA, 2019.
- [20] Y. Qin, N. Carlini, I. Goodfellow, G. Cottrell, and C. Raffel, "Imperceptible, Robust, and targeted adversarial examples for automatic speech recognition," in *ICML 2019*, 2019, pp. 9141–9150.
- [21] H. Yakura and J. Sakuma, "Robust Audio Adversarial Example for a Physical Attack," in *IJCAI 2019*. California: IJCAI 2019, aug 2019, pp. 5334–5341.
- [22] D. Wang, R. Wang, L. Dong, D. Yan, X. Zhang, and Y. Gong, "Adversarial examples attack and countermeasure for speech recognition system: A survey," in *International Conference on Security and Privacy in Digital Economy*. Springer, 2020, pp. 443–468.
- [23] F. Kreuk, Y. Adi, M. Cisse, and J. Keshet, "Fooling End-To-End Speaker Verification With Adversarial Examples," in *ICASSP 2018*, apr 2018, pp. 1962–1966.
- [24] Y. Gong and C. Poellabauer, "Crafting Adversarial Examples For Speech Paralinguistics Applications," in *Dynamic and Novel Advances in Machine Learning and Intelligent Cyber Security (DYNAMICS) Workshop*, San Juan, Puerto Rico, dec 2018.
- [25] D. Snyder, D. Garcia-Romero, G. Sell, D. Povey, and S. Khudanpur, "X-Vectors : Robust DNN Embeddings for Speaker Recognition," in *ICASSP 2018*, Alberta, Canada, apr 2018, pp. 5329–5333.
- [26] N. Dehak, P. J. Kenny, R. Dehak, P. Dumouchel, and P. Ouellet, "Front-end factor analysis for speaker verification," *IEEE Transactions on Audio, Speech, and Language Processing*, vol. 19, no. 4, pp. 788–798, 2010.
- [27] X. Li, J. Zhong, X. Wu, J. Yu, X. Liu, and H. Meng, "Adversarial Attacks on GMM I-Vector Based Speaker Verification Systems," in *ICASSP 2020*, Barcelona, Spain, may 2020, pp. 6579–6583.
- [28] Y. Xie, C. Shi, Z. Li, J. Liu, Y. Chen, and B. Yuan, "Real-Time, Universal, and Robust Adversarial Attacks Against Speaker Recognition Systems," in *ICASSP 2020*, may 2020, pp. 1738–1742.
- [29] J. Li, X. Zhang, C. Jia, J. Xu, L. Zhang, Y. Wang, S. Ma, and W. Gao, "Universal adversarial perturbations generative network for speaker recognition," in *2020 IEEE International Conference on Multimedia and Expo (ICME)*. IEEE, 2020, pp. 1–6.
- [30] Q. Wang, P. Guo, and L. Xie, "Inaudible adversarial perturbations for targeted attack in speaker recognition," *arXiv preprint arXiv:2005.10637*, 2020.
- [31] H. Abdullah, K. Warren, V. Bindschaedler, N. Papernot, and P. Traynor, "SoK: The Faults in our ASRs: An Overview of Attacks against Automatic Speech Recognition and Speaker Identification Systems," *arXiv:2007.06622 [cs]*, Jul. 2020, arXiv: 2007.06622. [Online]. Available: <http://arxiv.org/abs/2007.06622>
- [32] J. Villalba, Y. Zhang, and N. Dehak, "x-Vectors Meet Adversarial Attacks: Benchmarking Adversarial Robustness in Speaker Verification," p. 5.
- [33] Y. Zhang, Z. Jiang, J. Villalba, and N. Dehak, "Black-box Attacks on Spoofing Countermeasures Using Transferability of Adversarial Examples," p. 5.

- [34] N. Papernot, P. McDaniel, X. Wu, S. Jha, and A. Swami, "Distillation as a defense to adversarial perturbations against deep neural networks," in *2016 IEEE Symposium on Security and Privacy (SP)*. IEEE, 2016, pp. 582–597.
- [35] J. Buckman, A. Roy, C. Raffel, and I. Goodfellow, "Thermometer encoding: One hot way to resist adversarial examples," in *International Conference on Learning Representations*, 2018.
- [36] C. Guo, M. Rana, M. Cisse, and L. Van Der Maaten, "Countering adversarial images using input transformations," *arXiv preprint arXiv:1711.00117*, 2017.
- [37] Y. Song, T. Kim, S. Nowozin, S. Ermon, and N. Kushman, "Pixeldefend: Leveraging generative models to understand and defend against adversarial examples," *arXiv preprint arXiv:1710.10766*, 2017.
- [38] P. Samangouei, M. Kabkab, and R. Chellappa, "Defense-GAN: Protecting Classifiers Against Adversarial Attacks Using Generative Models," *arXiv:1805.06605 [cs, stat]*, May 2018, arXiv: 1805.06605. [Online]. Available: <http://arxiv.org/abs/1805.06605>
- [39] I. J. Goodfellow, J. Shlens, and C. Szegedy, "Explaining and harnessing adversarial examples," *arXiv preprint arXiv:1412.6572*, 2014.
- [40] A. Kurakin, I. Goodfellow, and S. Bengio, "Adversarial machine learning at scale," *arXiv preprint arXiv:1611.01236*, 2016.
- [41] A. Madry, A. Makelov, L. Schmidt, D. Tsipras, and A. Vladu, "Towards deep learning models resistant to adversarial attacks," *arXiv preprint arXiv:1706.06083*, 2017.
- [42] D. Zhang, T. Zhang, Y. Lu, Z. Zhu, and B. Dong, "You only propagate once: Painless adversarial training using maximal principle," *arXiv preprint arXiv:1905.00877*, vol. 2, no. 3, 2019.
- [43] A. Raghunathan, J. Steinhardt, and P. Liang, "Certified defenses against adversarial examples," *arXiv preprint arXiv:1801.09344*, 2018.
- [44] A. Levine and S. Feizi, "Wasserstein smoothing: Certified robustness against wasserstein adversarial attacks," in *International Conference on Artificial Intelligence and Statistics*. PMLR, 2020, pp. 3938–3947.
- [45] G. Chen, S. Chen, L. Fan, X. Du, Z. Zhao, F. Song, and Y. Liu, "Who is real bob? adversarial attacks on speaker recognition systems," *arXiv preprint arXiv:1911.01840*, 2019.
- [46] G. Rigoll and B. U. Seeber, "Mp3 compression to diminish adversarial noise in end-to-end speech recognition," in *Speech and Computer: 22nd International Conference, SPECOM 2020, St. Petersburg, Russia, October 7–9, 2020, Proceedings*, vol. 12335. Springer Nature, 2020, p. 22.
- [47] X. Li, N. Li, J. Zhong, X. Wu, X. Liu, D. Su, D. Yu, and H. Meng, "Investigating robustness of adversarial samples detection for automatic speaker verification," *arXiv preprint arXiv:2006.06186*, 2020.
- [48] A. Jati, C.-C. Hsu, M. Pal, R. Peri, W. AbdAlmageed, and S. Narayanan, "Adversarial Attack and Defense Strategies for Deep Speaker Recognition Systems," *arXiv:2008.07685 [cs, eess]*, Aug. 2020, arXiv: 2008.07685. [Online]. Available: <http://arxiv.org/abs/2008.07685>
- [49] M. Pal, A. Jati, R. Peri, C.-C. Hsu, W. AbdAlmageed, and S. Narayanan, "Adversarial defense for deep speaker recognition using hybrid adversarial training," *arXiv preprint arXiv:2010.16038*, 2020.
- [50] D. Snyder, D. Garcia-Romero, D. Povey, and S. Khudanpur, "Deep Neural Network Embeddings for Text-Independent Speaker Verification," in *INTERSPEECH 2017*, Stockholm, Sweden, aug 2017, pp. 999–1003.
- [51] J. Deng, J. Guo, N. Xue, and S. Zafeiriou, "ArcFace: Additive Angular Margin Loss for Deep Face Recognition," in *CVPR 2019*, 2019.
- [52] H. Zeinali, S. Wang, A. Silnova, P. Matějka, and O. Plchot, "But system description to voxceleb speaker recognition challenge 2019," *arXiv preprint arXiv:1910.12592*, 2019.
- [53] J. Villalba, N. Chen, D. Snyder, D. Garcia-Romero, A. McCree, G. Sell, J. Borgstrom, L. P. Garcia-Perera, F. Richardson, R. Dehak, P. A. Torres-Carrasquillo, and N. Dehak, "State-of-the-art speaker recognition with neural network embeddings in NIST SRE18 and Speakers in the Wild evaluations," *Computer Speech & Language*, vol. 60, p. 101026, mar 2020.
- [54] M. Tan and Q. Le, "Efficientnet: Rethinking model scaling for convolutional neural networks," in *International Conference on Machine Learning*, 2019, pp. 6105–6114.
- [55] A. Vaswani, N. Shazeer, N. Parmar, J. Uszkoreit, L. Jones, A. N. Gomez, L. Kaiser, and I. Polosukhin, "Attention is all you need," in *Advances in neural information processing systems*, 2017, pp. 5998–6008.
- [56] S.-M. Moosavi-Dezfooli, A. Fawzi, O. Fawzi, and P. Frossard, "Universal adversarial perturbations," in *Proceedings of the IEEE conference on computer vision and pattern recognition*, 2017, pp. 1765–1773.
- [57] M. Ravanelli and Y. Bengio, "Speaker recognition from raw waveform with sincnet," in *2018 IEEE Spoken Language Technology Workshop (SLT)*. IEEE, 2018, pp. 1021–1028.
- [58] A. Madry, A. Makelov, L. Schmidt, D. Tsipras, and A. Vladu, "Towards deep learning models resistant to adversarial attacks," in *International Conference on Learning Representations*, 2018.
- [59] J. Cohen, E. Rosenfeld, and Z. Kolter, "Certified adversarial robustness via randomized smoothing," in *International Conference on Machine Learning*, 2019, pp. 1310–1320.
- [60] K. Ren, T. Zheng, Z. Qin, and X. Liu, "Adversarial attacks and defenses in deep learning," *Engineering*, 2020.
- [61] D. Snyder, G. Chen, and D. Povey, "MUSAN: A Music, Speech, and Noise Corpus," 2015, arXiv:1510.08484v1.
- [62] T. Ko, V. Peddinti, D. Povey, M. L. Seltzer, and S. Khudanpur, "A study on data augmentation of reverberant speech for robust speech recognition," in *2017 IEEE International Conference on Acoustics, Speech and Signal Processing (ICASSP)*. IEEE, 2017, pp. 5220–5224.
- [63] M. Arjovsky, S. Chintala, and L. Bottou, "Wasserstein generative adversarial networks," in *Proceedings of the 34th International Conference on Machine Learning-Volume 70*, 2017, pp. 214–223.
- [64] C. Donahue, J. McAuley, and M. Puckette, "Adversarial Audio Synthesis," *arXiv:1802.04208 [cs]*, Feb. 2019, arXiv: 1802.04208. [Online]. Available: <http://arxiv.org/abs/1802.04208>
- [65] I. Gulrajani, F. Ahmed, M. Arjovsky, V. Dumoulin, and A. Courville, "Improved Training of Wasserstein GANs," *arXiv:1704.00028 [cs, stat]*, Dec. 2017, arXiv: 1704.00028. [Online]. Available: <http://arxiv.org/abs/1704.00028>
- [66] A. Athalye, N. Carlini, and D. Wagner, "Obfuscated gradients give a false sense of security: Circumventing defenses to adversarial examples," in *International Conference on Machine Learning*, 2018, pp. 274–283.
- [67] D. P. Kingma and M. Welling, "Auto-Encoding Variational Bayes," in *Proceedings of the International Conference of Learning Representations, ICLR 2014*, no. ML, Banff, Alberta, Canada, apr 2014, pp. 1–14. [Online]. Available: <http://arxiv.org/abs/1312.6114>
- [68] A. A. Alemi, I. Fischer, J. V. Dillon, and K. Murphy, "Deep variational information bottleneck," *ICLR 2017*, 2017.
- [69] D. J. Im, S. Ahn, R. Memisevic, and Y. Bengio, "Denoising criterion for variational auto-encoding framework," in *Proceedings of the Thirty-First AAAI Conference on Artificial Intelligence*, 2017, pp. 2059–2065.
- [70] R. Yamamoto, E. Song, and J.-M. Kim, "Parallel wavegan: A fast waveform generation model based on generative adversarial networks with multi-resolution spectrogram," in *ICASSP 2020-2020 IEEE International Conference on Acoustics, Speech and Signal Processing (ICASSP)*. IEEE, 2020, pp. 6199–6203.
- [71] V. Panayotov, G. Chen, D. Povey, and S. Khudanpur, "Librispeech: An asr corpus based on public domain audio books," in *2015 IEEE International Conference on Acoustics, Speech and Signal Processing (ICASSP)*, 2015, pp. 5206–5210.
- [72] G. R. Doddington, "The NIST speaker recognition evaluation - Overview, methodology, systems, results, perspective," *Speech Communication*, vol. 31, no. 2-3, pp. 225–254, jun 2000. [Online]. Available: [http://dx.doi.org/10.1016/S0167-6393\(99\)00080-1](http://dx.doi.org/10.1016/S0167-6393(99)00080-1)
- [73] A. Paszke, S. Gross, F. Massa, A. Lerer, J. Bradbury, G. Chanan, T. Killeen, Z. Lin, N. Gimelshein, L. Antiga, A. Desmaison, A. Kopf, E. Yang, Z. DeVito, M. Raison, A. Tejani, S. Chilamkurthy, B. Steiner, L. Fang, J. Bai, and S. Chintala, "PyTorch: An Imperative Style, High-Performance Deep Learning Library," in *NeurIPS 2019*. Curran Associates, Inc., 2019, pp. 8024–8035.
- [74] A. Nagrani, J. S. Chung, W. Xie, and A. Zisserman, "Voxceleb: Large-scale speaker verification in the wild," *Computer Speech and Language*, vol. 60, 2020.
- [75] W. Shi, J. Caballero, F. Huszár, J. Totz, A. P. Aitken, R. Bishop, D. Rueckert, and Z. Wang, "Real-time single image and video super-resolution using an efficient sub-pixel convolutional neural network," in *Proceedings of the IEEE conference on computer vision and pattern recognition*, 2016, pp. 1874–1883.
- [76] J. Kominek and A. W. Black, "The cmu arctic speech databases," in *Fifth ISCA workshop on speech synthesis*, 2004.
- [77] J. S. Chung, A. Nagrani, and A. Zisserman, "Voxceleb2: Deep speaker recognition," *arXiv preprint arXiv:1806.05622*, 2018.